Bifunctionalization of Cellulose Fibers by One-Step Williamson's Etherification to Obtain Modified Microfibrillated Cellulose

Céline Moreau, Xavier Falourd, Malika Talantikite, Bernard Cathala, Ana Villares

Bifunctionalization of Cellulose Fibers by One-Step Williamson's Etherification to Obtain Modified Microfibrillated Cellulose

Céline Moreau, Xavier Falourd, Malika Talantikite, Bernard Cathala, and Ana Villares*

ACCESS | Metrics & More | Article Recommendations | Supporting Information

ABSTRACT: We present here a straightforward strategy to prepare multifunctional cellulose by a one-pot modified carboxymethylation reaction. We focused on the introduction of negative charge (carboxymethyl groups) and benzophenone moieties {[4-(bromomethyl)phenyl][4-(prop-2-yn-1-yloxy)phenyl]methanone} on the surface of cellulose fibers by a concomitant Williamson's etherification. The presence of negative charge on the cellulose surface facilitated fibrillation, and we obtained microfibrillated cellulose by soft magnetic stirring. The chemical grafting of benzophenone functionalities was evidenced by combining Fourier-transform infrared and solid-state ^{13}C CP/MAS NMR techniques and by the polymerization of different monomers (methyl methacrylate, dodecyl methacrylate, and styrene) on the cellulose surface. The presence of both functionalities allowed fabricating papers and 3D networks, and their subsequent cross-linking by the carboxylate groups, and hydrophobization by polymerization at the benzophenone groups. Indeed, bifunctional cellulose showed interesting properties that were not achieved by the mixture of monofunctional celluloses.

KEYWORDS: carboxymethylation, fibrillation, cellulose nanofiber, cellulose microfiber
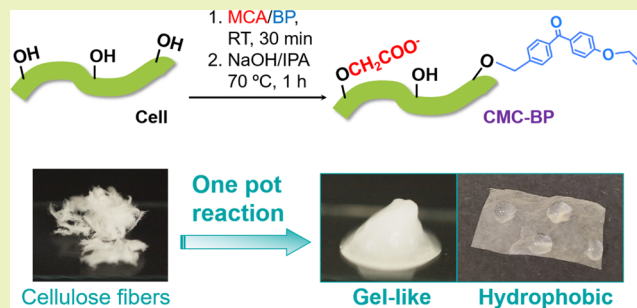
INTRODUCTION

Micro- and nanofibrillated cellulose has attracted much interest scientifically and commercially because of its attractive properties such as high aspect ratio, high strength and stiffness, low density, transparency, high surface area, and low thermal expansion.[1−3] The mentioned properties together with high abundancy, renewability, and recyclability, have triggered the fabrication and commercialization of nanofibrillated cellulose (CNF) for a wide range of applications including packaging, paper and board, composite materials, adhesives, absorbents, electronics, medical, pharmaceutical, and cosmetic products.[4]

Despite their outstanding properties, nanocelluloses remain underemployed because of several constraints associated to their manufacture. Generally, cellulose fibers are disintegrated into fine fragments, or cellulose nanofibers, by mechanical refining methods. However, these procedures involve high-energy consumption and they tend to damage the nanofiber structure by reducing molar mass and crystallinity.[5] Different pretreatments have been developed to facilitate the refining process, such as mild enzymatic hydrolysis, fiber oxidation catalyzed by the 2,2,6.6-tetramethylpiperidine-1-oxyl (TEMPO) radical, or carboxymethylation reactions.[6] Enzymatic pretreatment involves the use of endoglucanases or cellulase cocktails that disrupt the cellulose structure facilitating fibrillation; however, the energy required for shear forces is still high and multiple passes through the homogenizer are required.[7,8] The TEMPO-catalyzed oxidation

was proposed as one of the most promising methods for the production of cellulose nanofibers.[9,10] Indeed, TEMPO selectively transforms primary hydroxyls at C6 on cellulose fiber surface into carboxylate groups, which create electrostatic repulsions and facilitate the separation of cellulose nanofibers.[11] The use of the TEMPO oxidation may reduce the energy cost but results in high quantities of toxic wastes, and the degree of polymerization may be reduced during oxidation.[12−14] Therefore, a significant scientific and technologic challenge in the use of nanocelluloses arises from the exploration of novel sustainable approaches for their preparation procedure that reduce energy consumption. Traditionally developed for the complete solubilization of the cellulose fiber,[15,16] controlled carboxymethylation can be viewed as a strategy to facilitate fibrillation. Thus, to avoid the complete solubilization, fibers are first impregnated with monochloroacetic acid (MCA), and then, the hydroxyl groups are activated by concentrated NaOH solutions to perform Williamsom etherification on the hydroxyl groups.[17,18] The degree of substitution (DS), which is the average number of
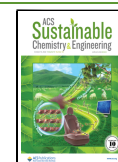
functional groups introduced in the cellulose polymer, can be controlled by experimental conditions (MCA and NaOH ratios, temperature and reaction time).[19] Despite the versatility of carboxymethylation, this strategy is scarcely used for the preparation of CNF at the industrial level. One of the main drawbacks relied on the solvent exchange to isopropanol (IPA); however, recent studies have revealed that never dried fibers can be carboxymethylated without any step of solvent exchange, only by simply filtrating them.[20]

Another bottleneck on the commercialization of CNF relies on the ability to adapt their properties to industrial applications. For instance, the introduction of functional groups that modify the nature of interactions (hydrogen bonds, electrostatic, and hydrophobic) or the polarity from hydrophilic to hydrophobic favors better dispersion of nanocelluloses for the fabrication of composites or for their use as emulsion stabilizers in water in oil (w/o) or oil in water (o/w) systems.[21] To increase commercial applications, such as composites, coatings, or packaging, the functionalization of CNF would therefore require chemical modifications after fibrillation, which generally increases costs and environmental impact.

In this work, we performed concomitant Williamson etherifications to multifunctionalize the surface of the cellulose fiber. We performed a bifunctionalization with carboxymethyl groups and benzophenone moieties in a 1 h reaction. The presence of negative charge from carboxymethyl groups facilitated fiber disruption to the micrometric scale, thus reducing the energy required for fibrillation. Benzophenone functionalities allowed the surface polymerization to fabricate hydrophobic materials.

■ EXPERIMENTAL SECTION

Materials. Delignified bleached softwood Kraft pulp was used as the starting cellulose material. It was kindly provided by the Centre Technique du Papier (CTP, Grenoble, France). Monochloroacetic acid (MCA), [4-(bromomethyl)phenyl][4-(prop-2-yn-1-yloxy)-phenyl]methanone (BP), sodium hydroxide, methyl methacrylate, dodecyl methacrylate, styrene, tetrahydrofuran (THF), and ferric chloride were purchased from Sigma-Aldrich (France) and used without further purification. Isopropanol (IPA) and diethyl ether were supplied by VWR International (France).

General Procedure for Bifunctionalization. Cellulose fibers (100 mg) were first dispersed in water with a blender. The fibers were filtrated using a vacuum filtration system (PVDF membranes, 0.22 μm, Durapore). The fibers were then impregnated with MCA (10 mg, 0.10 mmol) dissolved in 0.5 mL of IPA for 30 min at room temperature. MCA is toxic, so it must be handled with under a fume hood and the operator must wear protective gloves and clothing and eye protection. Then, BP (10 mg, 0.03 mmol) dissolved in diethyl ether (2 mL) was added to the fibers and impregnated for 30 min at room temperature. After impregnation, fibers were added to a heated solution (60 °C) of sodium hydroxide (16 mg, 0.4 mmol) in IPA (1 mL) in a two-neck round-bottom flask. 2.5 mL of IPA was added to achieve a total IPA reaction volume of 5 mL. The reaction was allowed to proceed for 60 min at 70 °C under reflux. Fibers were purified by filtration (PVDF membranes, 0.22 μm, Durapore) and washing steps with IPA (×3) and water (×3) until reaching neutral pH.

Polymerization on the Cellulose Surface. Fibers functionalized with BP were submitted to the polymerization of different monomers (methyl methacrylate, dodecyl methacrylate, and styrene). For this purpose, 5 mg of functionalized fibers were incubated with monomers (0.2 mmol) under UV light (365 nm, UV lightning cure, 4500 mW cm^{-2}) for 1 h. Excess of monomers were removed by thorough washing with THF and water.

Fabrication of Cellulose Materials. Three-dimensional networks were prepared by freezing at −20 °C 1 g of benzophenone-modified cellulose dispersions at 2% w/v (20 mg of dry mass) in test tubes (diameter 1 cm) for 1 h.[22] Freezing favored the interaction between fibers and allowed the formation of 3D networks on a tube.

Papers were prepared by the filtration of 10 mL of benzophenone-modified cellulose dispersions at 5 g L^{-1} (50 mg) through 0.22 μm. Filtration was performed at 300 mbar for 30 min. Then, papers were pressed at 1 bar by a pneumatic sheet press (Regmed, Press SP-21) and dried by a speed dryer (Rycobel group model 145) at 40 °C for 2 h. Paper thickness was measured by a micrometer, and density was calculated by weighting the dried papers.

Papers and networks were cross-linked by the addition of 1 mL of FeCl$_3$ at 0.001 M.

Characterization. *Optical Microscopy.* Cellulose samples (0.1 g L^{-1} in Milli-Q water) were deposited onto a glass slide, dried at 40 °C, and observed by a BX51 polarizing microscope (Olympus France S.A.S.) with a 4× objective. Images were captured by a U-CMAD3 camera displaying a U-TV0.5XC-3 adaptor (Olympus Japan).

Rheology. Rheological measurements were performed using stress-controlled rheometer AR-2000 (TA Instruments). Plate geometry (40 mm) was selected. All measurements were performed at 20 °C. Samples were covered with paraffin oil to prevent evaporation during measurements. The elastic (G') and viscous (G'') moduli were measured within the linear response regime. Measurements were performed twice and the average of values is reported in the graphs.

Infrared Analysis (FT-IR). Infrared spectra were recorded from KBr pellets containing freeze-dried cellulose samples placed directly in a Nicolet iS50 FTIR spectrometer (Thermo Scientific) in the absorbance mode. All spectra were recorded with a 4 cm^{-1} resolution after 200 continuous scans from 400 to 4000 cm^{-1}.

Conductometry. The surface charge was measured by conductometric titration with a 0.01 M NaOH solution by a TIM900 titration manager and a CDM230 conductometer equipped with a CDC749 conductivity cell. The DS was then calculated by the following expression[23]

$$DS = \frac{n_{COOH}162}{m_{fibers} - n_{COOH}58} \tag{1}$$

where n_{COOH} is the number of equivalents of COOH calculated from conductometric titration, m_{fibers} is the mass of pulp (dry basis), 162 accounts for the molecular weight of the anhydroglucose unit of cellulose, and 58 is the net increase in the weight of the anhydroglucose unit of cellulose for each sodium carboxymethyl group substituted.

Solid-State ^{13}C CP/MAS NMR. Cellulose samples (100 mg) were rehydrated in 50 μL of H$_2$O and water excess was removed using an adsorbent. About 80−100 mg of each sample was packed into a 4 mm NMR rotor. Cross-polarization magic angle spinning (CP/MAS) NMR experiments were acquired on a Bruker AVANCE III 400 spectrometer operating at a ^{13}C frequency of 100.62 MHz equipped with a double resonance H/X CP/MAS 4 mm probe. Measurements were conducted at room temperature with a MAS spinning rate of 12 kHz. The CP pulse sequence parameters were as follows: 2.5 μs proton 90° pulse, 2 ms CP contact time at 67.5 kHz, and 10 s recycle time. The number of accumulations for the CP/MAS ^{13}C spectra was typically 2048 scans. ^{13}C NMR spectra were referenced to the carbonyl peak of glycine at 176.03 ppm. All "cellulosic" spectra were processed with Gaussian multiplication parameters of LB = −5 Hz and GB = 0.1. NMR spectra were deconvoluted as previously described.[24,25]

Values of crystallinity, accessible surface (AS), inaccessible surface (IAS), accessible/total fibril surface ratio [AS/(AS + IAS)], lateral fibril dimensions (LFDs), and lateral fibril aggregate dimensions (LFADs) (assuming 0.57 nm for cellulose chains width) were calculated from peak deconvolution of the C4 region (∼77−91 ppm) based on the previously described method.[26−28]

Scheme 1. Reaction Schemes of Monofunctionalization Reactions (a, Carboxymethylation; c, Introduction of Benzophenone), and b, One Pot Carboxymethylation and Introduction of Benzophenone on the Cellulose Fiber Surface[a]
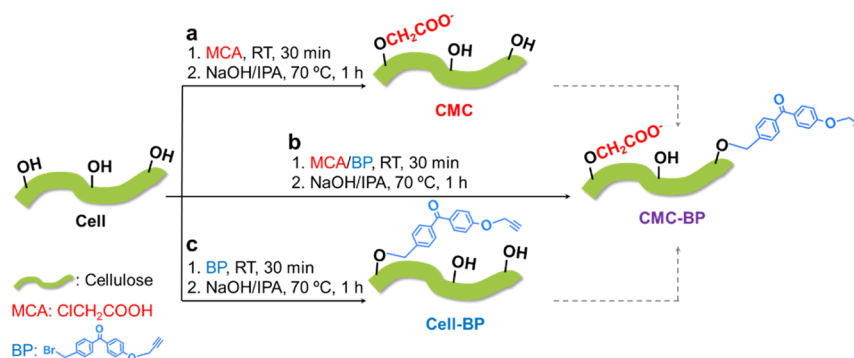
[a]In the scheme, CNFs are represented as green rods. Dimensions of CNF, MCA, and BP are not to scale.
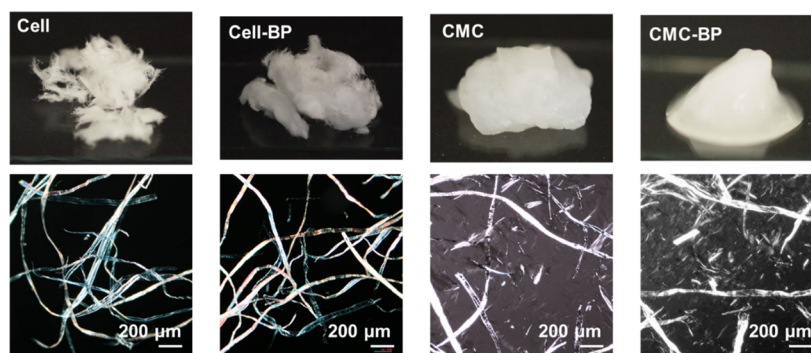

Figure 1. Visual aspect and optical microscopy images of native cellulose fibers (Cell), benzophenone-functionalized cellulose fibers (Cell-BP), CMC, and CMC-BP.

Solid-state ^{13}C CP/MAS NMR of BP powder was also acquired as for previous samples using a contact time of 3 ms and was processed with LB = 30 Hz and GB = 0.1.

Contact Angle. The static contact angle of water on papers was measured by means of a Digidrop Contact Angle Meter (GBX Scientific Instruments, Dublin, Ireland) using the sessile drop method. A 5 μL water drop was made on the tip of a syringe and placed on the substrate surface by moving the substrate vertically until contact was made between the drop and the sample. High-resolution images of the droplets were captured via a video camera and Digidrop software was used for data collection and analysis. Five individual measurements were obtained for each set of data and the average values are calculated.

■ RESULTS AND DISCUSSION

In this work, we present a modified carboxymethylation procedure to achieve one-pot fibrillation and functionalization of cellulose fibers in a 1 h reaction. Carboxymethylation of cellulose fibers commonly involves solvent exchange from fiber aqueous suspensions to ethanol and then to IPA,[18] so huge amounts of ethanol are consumed during this step. Recently, Im et al.[20] demonstrated that filtration could replace the solvent exchange step providing that the water content in the reaction medium is below 4.0% (w/v). Therefore, we filtrated delignified bleached softwood Kraft pulp to a fiber consistency of 20% (w/v). Then, the conventional carboxymethylation reaction was modified by introducing an additional step of fiber impregnation with the desired functionality. Thus, the pulp was impregnated for 30 min with MCA and BP in IPA and then allowed to react in an alkaline medium (Scheme 1).

The introduction of negative charges by the carboxymethyl groups created electrostatic repulsions between the fibrils, which facilitated fibrillation, resulting in gel-like dispersions. For the purpose of comparison, fibers were separately impregnated with MCA (Scheme 1a) or BP (Scheme 1c) to introduce only one functionality (carboxymethyl or benzophenone). Figure 1 shows the aspect and microscopy images of native cellulose fibers (Cell), benzophenone-functionalized cellulose fibers (Cell-BP), carboxymethylated cellulose (CMC), and benzophenone-functionalized carboxymethyl cellulose (CMC-BP).

The introduction of benzophenone functionalities (Cell-BP) did not significantly modify the fiber morphology compared to native fibers (Cell). On the contrary, the visual aspect and microscopy images showed gel aspect and fiber disruption for carboxymethylated samples (CMC and CMC-BP). The introduction of negative charge by the carboxymethyl groups facilitated the separation between the microfibrils and the subsequent fibrillation, which yielded a gel-like behavior. Fibrillation was achieved by magnetic stirring overnight without any further mechanical treatment, which demonstrated the potential of our protocol to fabricate functionalized CNF in one step.

The presence of functionalities was demonstrated by FT-IR (Figure 2). The spectrum of pure BP was also recorded to better identify the peaks.

The spectra showed the characteristic profile of cellulose fibers.[29] When looking in detail the 1800−1500 cm^{-1} region, it was evident that new peaks appeared from functionalization. Carboxymethylation was demonstrated by the appearance of a
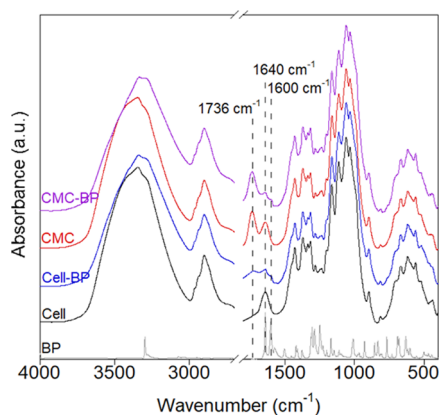
Figure 2. FT-IR spectra of native cellulose fibers (Cell), benzophenone-functionalized cellulose fibers (Cell-BP), CMC, CMC-BP, and BP registered at acid pH.

new band at 1736 cm^{-1}, corresponding to the C=O stretch from the carboxylic acid group.[30] This band was clearly detected on both CMC and CMC-BP. The pure benzophenone derivative presented an intense band at 1640 cm^{-1}, ascribed to the ketonic C=O, which is a distinctive band belonging to benzophenone.[31,32] The BP bands were detected on both benzophenone-functionalized samples (Cell-BP and CMC-BP). The presence of the band at 1640 cm^{-1} was not very clear because it overlapped the symmetric deformation vibration of adsorbed water molecules band at 1635 cm^{-1}.[29] Nevertheless, the stretching vibration of C=C bonds in the aromatic rings at 1600 cm^{-1} unambiguously demonstrated the presence of benzophenone moieties in Cell-BP and CMC-BP.[33,34] Another feature of Fourier-transform infrared (FTIR) spectra that suggested the chemical bond of benzophenone moieties was the modification of the OH vibration region (3000−3800 cm^{-1}). Hence, the relative intensity of the band at 3310−3230 cm^{-1}, ascribed to intermolecular hydrogen bonds of 6-OH···O3′,[35] increased in Cell-BP and CMC-BP, suggesting that the hydrogen bonding pattern was modified by the benzophenone linkage. When cellulose fibers and BP were just mixed without performing the Williamson etherification, the FTIR spectrum did not show any change in the hydrogen bonding pattern, only a small peak from benzophenone at 3297 cm^{-1} was observed (Figure S1, green line). Then, FTIR spectra demonstrated that the purification of cellulose fibers by filtration, as performed after the reaction of functionalization, removed completely benzophenone (Figure S1, pink line). The introduction of the two functionalities was therefore demonstrated by the detection of bands corresponding to both carboxymethyl and benzophenone groups in the CMC-BP spectrum. Furthermore, from Figure 2, the intensity of the carboxyl group was similar for both CMC and CMC-BP samples, which suggested that the DS of the carboxymethylation reaction was not impacted by the simultaneous reaction with the benzophenone derivative.

The carboxymethylated samples were then analyzed by conductometric titration to determine the carboxyl content after functionalization. The total charge of native cellulose fibers (Cell) was 0.218 ± 0.024 mmol g^{-1}. The total charge of CMC was 0.745 ± 0.019 mmol g^{-1}, which corresponded to a DS of 0.13 ± 0.01. This value was slightly higher than previous values reported in the literature.[18,20] When fibers were simultaneously carboxymethylated and functionalized with benzophenone, the total charge was 0.709 ± 0.037 mmol g^{-1}, and the corresponding DS was 0.12 ± 0.01. In previous studies, Kaldéus et al.[36] observed that MCA and alkyl halides were competing reactions. Hence, if pulp was simultaneously impregnated with both chemicals, extremely low values of total fiber charge were obtained. Therefore, their protocol involved a first carboxymethylation reaction followed by the etherification with allyl bromide or propargyl bromide. In their conditions, the second etherification required much higher amounts of alkyl halides (5:1 molar equiv to the anhydroglucose units) compared to the low amounts of benzophenone derivatives we used in our protocol (0.04:1 molar equiv). Indeed, we did not observe a significant decrease in the total charge nor in the FTIR intensity of benzophenone bands when both reactions occurred concurrently, which indicated that both functionalities were present on the cellulose surface.

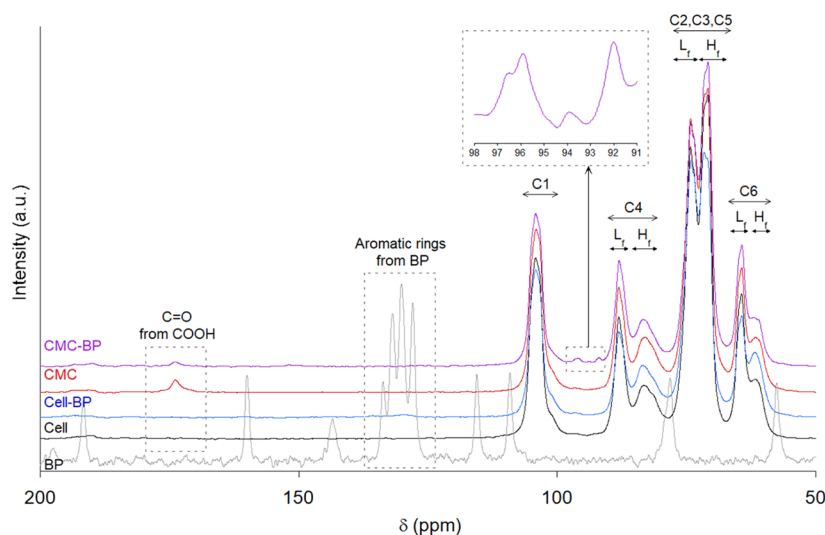**Figure 3.** Solid-state ^{13}C CP/MAS NMR spectra of native cellulose fibers (Cell), benzophenone-functionalized cellulose fibers (Cell-BP), CMC, CMC-BP, and BP with specific peak regions corresponding to C1, C4, C2, C3, C5, and C6.[37,38] For C4 and C6 and C2, C3, and C5 regions, two peak groups are observed and noted H$_f$ and L$_f$ for their chemical shift positions at high field and low field, respectively.

Solid-state ^{13}C CP/MAS NMR experiments were performed to investigate any change on cellulose due to carboxymethylation and/or BP functionalization (Figure 3).

The spectrum of unmodified fibers (Cell) displayed the characteristic resonances of cellulose between 55 and 110 ppm: C1 at δ 100−108 ppm, C4 at δ 79−90 ppm, C2, 3, 5 at δ 68−78 ppm, and C6 at δ 58−67 ppm.[37,38] Two distinct peak groups were observed from C4, C6, one part at high field (H_f) and the other one at low field (L_f), which corresponded to carbons at ordered and less-ordered cellulose, respectively.[28,37] More specifically, signals from C4 carbons at L_f position (∼87−89 ppm) corresponded to crystalline forms (including paracrystalline), while C4 carbons at H_f position (∼82−84 ppm) represented the less ordered forms of cellulose. Also, the overlapping peaks located at 70−78 ppm could be assigned to C3−C5 carbons at L_f (∼73−75 ppm) and to C5−C2 carbons at H_f (∼70−72 ppm).[39]

Functionalization of cellulose fibers did not significantly modify the profile of the ^{13}C NMR spectrum of cellulose fibers from 50 to 105 ppm. CMC clearly presented a peak at ∼174 ppm ascribed to carboxyl carbon; this peak was also observed in the CMC-BP spectrum but with lower intensity.[40] CMC-BP spectrum also presented several peaks of very low intensities at the δ 90−96 ppm, that have been previously observed and related to cellulose oxidation.[41] The spectrum of BP alone showed distinct ^{13}C peaks from 50 to 200 ppm with the characteristic peaks from the aromatic rings at 120−125 ppm and the carbonyl at 192 ppm.[42] These BP peaks were slightly detected in Cell-BP and not detected in the CMC-BP spectrum because the DS was low (estimated at 0.005 from the ^{13}C NMR areas). Also, due to the inherent broad signals of cellulose in the "solid" state, the ^{13}C NMR spectrum did not allow the detection of small signals from the BP functionalities. Generally, the functionalities on the cellulose fibers are not observed by ^{13}C NMR if the DS is below 0.2. For example, Kaldéus et al.[36] did not observed noticeable changes in the NMR spectra after allyl or alkyne functionalization when DS was around 0.0018−0.016. On the contrary, at DS above 0.3, it is possible to detect the peaks corresponding to the grafted functionality, such as aromatic carboxylic acids (DS ≈ 0.3−0.5)[43] or α-acyloxycarboxamide, methacrylic acid, and pentynoic acid (DS ≈ 0.7).[44] At high DS (0.7−3), the introduction of carboxymethyl groups at 2-, 3-, or 6-position yields downfield chemical shifts (8.6−9.0 ppm) for the directly attached carbons (β-effect, through two bonds), whereas γ- and δ-effects (through three and four bonds) are very small.[45,46] When the DS is low (<0.2), the signal shifts could be overlapped with the bands of unmodified cellulose, so that their detection is difficult, if not impossible.

Therefore, spectral deconvolution of the C4 region was performed based on our previous works in order to reveal any structural change associated to the chemical grafting and to determine the crystallinity and fibril dimensions.[24,25] Details of deconvoluted peaks are showed in Figure S2. Crystallinity index (CI) was calculated based on the NMR signal areas from crystalline part (∼86−91 ppm) over the total signal surface of the C4 region (Table 1). Crystallinity of native cellulose fibers (∼54%) was in agreement with previous values obtained for cellulose pulps containing hemicelluloses.[25]

When cellulose fibers were functionalized with benzophenone, there was a decrease in crystallinity, from 54.2 ± 1.2% (Cell) to 44.1 ± 0.3% (Cell-BP), which suggested that the crystalline regions could be disrupted by the BP-functionaliza-

Table 1. Values of CI, LFD, LFAD, and Accessible/Total Fibril Surface Ratio [AS/(AS + IAS)] Calculated from the C4 Region Deconvolution of the Solid-State ^{13}C CP/MAS NMR Spectra of Native Cellulose Fibers (Cell), Benzophenone-Functionalized Cellulose Fibers (Cell-BP), CMC, and CMC-BP[a]

sample	CI (%)	LFD (nm)	LFAD (nm)	AS/(AS + IAS) ratio
Cell	54.2 ± 1.2	4.3 ± 0.1	19.5 ± 0.1	29.2 ± 1.1
Cell-BP	44.1 ± 0.3	3.4 ± 0.1	14.3 ± 0.1	30.3 ± 1.1
CMC	54.1 ± 0.6	4.3 ± 0.2	15.4 ± 0.2	38.0 ± 1.3
CMC-BP	59.7 ± 1.3	5.0 ± 0.2	24.4 ± 3.9	26.2 ± 0.8

[a]Results are expressed as mean ± standard deviation.

tion. Considering that crystallinity represents the core-to-volume ratio of the crystallite,[47] the BP-functionalization seemed to increase the specific surface area. This change in crystallinity was not observed for carboxymethylation because CMC presented a crystallinity of 54.1 ± 0.6%. However, when cellulose contained both functionalities (CMC-BP), crystallinity increased to 59.7 ± 1.3%, probably due to the removal of less ordered regions, and the decrease of volume of the crystallite.

LFD and LFAD were also estimated from NMR spectra (Table 1). The values agreed well with previous results reported.[25,48] The functionalization with benzophenone resulted in a clear decrease in both LFD and LFAD for Cell-BP compared to Cell, which pointed to a more compact arrangement of fibrils. The accessible/total fibril surface ratio [AS/(AS + IAS)] did not significantly change due to both increase of IAS and AS, that is, the disordered regions of cellulose fibrils; indeed, as IAS increases, the values of crystallinity and LFD decrease.[25,49] Also, this strongly impacts the value of LFAD dimensions. The lower LFD of Cell-BP could be ascribed to fiber shrinkage and the subsequent contraction after reaction. On the contrary, when cellulose fibers were carboxymethylated (CMC), there was no change in LFD (4.3 ± 0.2 nm), whereas LFAD decreased from 19.5 ± 0.1 to 15.4 ± 0.2 nm, probably due to the fibril separation because of electrostatic repulsion between the negatively charged carboxymethyl groups. This assumption was confirmed by the increase of the AS/(AS + IAS) ratio to 38.0 ± 1.3, as a consequence of the decrease of IAS, and therefore the fibril separation. When both functionalities were introduced in the fiber (CMC-BP), LFD increased slightly, whereas LFAD increased significantly. The higher LFD could be explained by the repulsion between cellulose chains and the subsequent swelling. The high LFAD value obtained for CMC-BP (24.4 ± 3.9 nm) pointed to fibril aggregation, where aggregates could be formed by a higher number of fibrils. This was confirmed by the lower AS/(AS + IAS) ratio (26.2 ± 0.8), which indicated that AS became IAS, together with the increase in crystallinity, which suggested that disordered regions were removed resulting in an ordered pattern.

To go further in spectra analysis, we determined the changes of peak areas in the C6 and C2, C3, and C5 regions as compared to peak areas of cellulose fibers (Cell). The relative areas from carbons at high field (H_f ∼59−62 ppm) and carbons at low field (L_f ∼63−64 ppm) at C6 revealed a high increase of H_f (+27%) to the detriment of L_f (−20%) for Cell-BP compared to Cell (100%). Comparing CMC and CMC-BP, a similar H_f increase was observed, but in a lower extent

(+8%). At the C2, C3, and C5 regions, two peak groups were distinguished, which can be assigned to C3/C5 carbons at L_f (69−71 ppm) and C5/C2 carbons at H_f (72−74 ppm).[39] For Cell-BP, the relative areas of L_f peaks corresponding to C3/C5 increased (+9%), whereas the H_f peaks corresponding to C5/C2 decreased (−9%). On the contrary, CMC-BP showed the opposite behavior, the areas from L_f peaks decreased (−5%) and areas from H_f peaks increased (+3%). The variation in the relative areas of each region suggested a preferential interaction of BP to the C3/C5 and C6 carbons, which could point to chemical grafting at C3 and/or C6 positions. The differences between Cell-BP and CMC-BP could be ascribed to the competition between carboxymethyl and benzophenone functionalities, so the presence of carboxymethyl groups could modify the substitution pattern of BP.

The presence of charge from carboxymethyl groups improved the colloidal stability and facilitated the fibrillation. When fibrillation is attained at a nanometric scale, mechanical and viscoelastic properties are impacted and dispersions are characterized by gel behavior. We used dynamic rheology to assess the properties of CMC-BP dispersions and characterize the gel behavior. Classical viscous fluids present storage modulus (G') values lower than loss modulus (G''), whereas ideal gels are characterized by storage modulus independent of frequency, and G' greater than G''.[7] On the basis of Figure 4, a
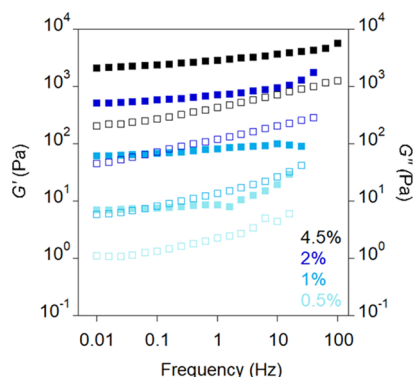

Figure 4. Storage modulus (G') (solid squares) and loss modulus (G'') (hollow squares) as a function of frequency for CMC-BP dispersions at different concentrations (0.5−4.5%).

gel-like behavior ($G' > G''$) was observed for the concentration range studied (0.5−4.5%). The obtained values were in agreement with those observed for enzymatically prepared microfibrillated cellulose.[7] Both G' and G'' increased with concentration, which clearly demonstrated the formation of an entangled network structure.

Benzophenone is one of the most well-known photo-initiators for radical polymerization. Benzophenone abstracts hydrogen from H-donors such as monomers, and forms two types of radicals: a ketyl radical on the benzophenone moiety and an alkyl radical generated on the H-donor that starts polymerization.[50] Therefore, the benzophenone functionalities grafted on the cellulose surface acted as initiators to grow polymer chains on the cellulose surface. The resultant polymers are therefore tethered by one chain end to the cellulose surface and can adopt various conformations depending on grafting density.[51] We studied three different monomers, methyl methacrylate, dodecyl methacrylate, and styrene, and polymerization was achieved by UV irradiation. The growth of hydrophobic uncharged polymer chains was

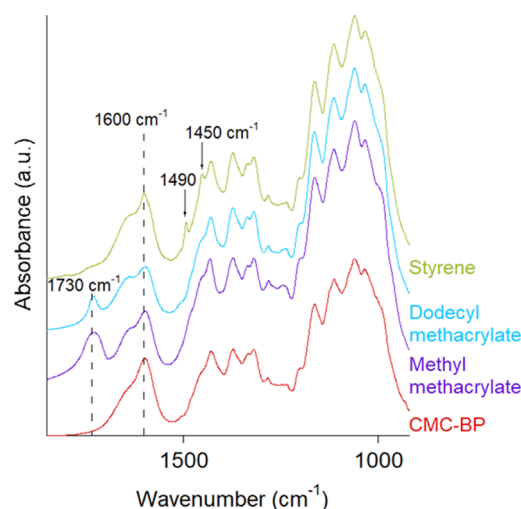monitored by FT-IR (Figure 5). The full spectra are showed in Figures S3−S5.

Figure 5. FT-IR spectra of CMC-BP before and after incubation with methyl methacrylate, dodecyl methacrylate, and styrene monomers.

When native cellulose fibers were incubated with the monomers, after washing with THF and water, the FT-IR spectrum did not show any trace of any of the monomers (Figures S3−S5), which indicated that the monomer was chemically grafted and not adsorbed on the fiber surface. On the contrary, the FT-IR spectra of Cell-BP and CMC-BP showed the presence of new bands, corresponding to the polymer growth. As the samples were not acidified, the carboxylate (COO^-) from the carboxymethyl group appeared at 1600 cm^{-1}. For polymethacrylates (methyl and dodecyl), the new band at 1730 cm^{-1} was ascribed to the carbonyl group from the acrylate. Finally, the polymerization of styrene was demonstrated by the presence of bands at 1450, 1490, and 1585 cm^{-1} corresponding to the C−H aromatic stretching.

Zoppe et al. observed that anionic surface sulfate half-ester groups had an effect on the surface initiator efficiency in aqueous surface initiated atom transfer radical polymerization (SI-ATRP).[52] Specifically, in Cu-mediated SI-ATRP, electrostatic interactions likely caused the overall enrichment of catalytic species (copper) at highly charged CNC interfaces leading to higher initiator efficiency. However, the high surface charge density led to lower molecular weight and higher polydispersity of poly(N,N-dimethylacrylamide) brushes. Overall, the carboxymethyl surface charge of CMC-BP could offer a means to further manipulate polymerization to rapidly obtain the desired molecular weight and polydispersity. The characterization of polymer chains synthesized at the cellulose surface was out of the scope of this work.

The polymerization at the benzophenone functionalities was performed to establish the proof of concept of the advantages of bifunctionalized cellulose. The presence of both functionalities on the same fiber (CMC-BP) provided interesting properties that could not be achieved by the mixture of monofunctionalized celluloses (Cell-BP and CMC). Hence, we fabricated three-dimensional networks by freezing Cell-BP, CMC-BP, and a 1:1 mixture of Cell-BP and CMC on test tubes.[22] In order to avoid their dispersion in water, 3D networks were reticulated with Fe^{3+} ions to achieve ionic cross-link between the carboxylate groups.[53] Figure 6A shows the
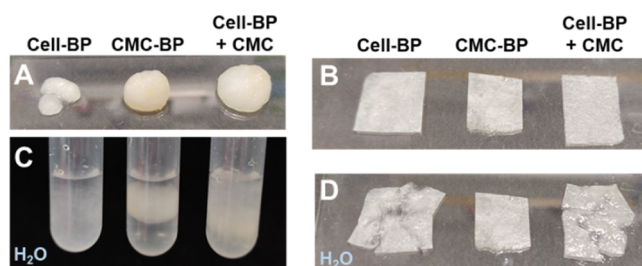
Figure 6. Photographs of 3D networks (A,C) and papers (B,D) of Cell-BP, CMC-BP, and a mixture of Cell-BP and CMC cross-linked with Fe^{3+} ions (A,B), and after their swelling in water (C,D).

photographs of the 3D networks. In the case of Cell-BP, the absence of carboxylates prevented the reticulation and therefore the network was not stable and it was broken when it was extracted from the tube. When samples were immersed in water, only the CMC-BP sample was stable and kept its shape (Figure 6C). The mixture Cell-BP and CMC showed a separation between cross-linked CMC and Cell-BP that disrupted the network and favored its dispersion in water.

Similarly, we fabricated papers with Cell-BP, CMC-BP, and a mixture of Cell-BP and CMC by vacuum filtration. The water removal favored the interaction between cellulose fibers and the three dried papers were freestanding after their preparation. The thickness was 61.3 ± 4.2 μm and the grammage was in all cases 46.7 ± 1.3 g m^{-2}. Then, papers were immersed in Fe^{3+} solution in order to promote cross-linking through carboxylate groups by the same procedure used for the 3D networks. After immersion in water, only the CMC-BP paper was water-resistant. Similarly to the results obtained for the 3D networks, in the case of the mixture of Cell-BP and CMC, the cross-linking between the carboxymethyl groups of CMC was not enough to maintain the paper structure and the dispersion of Cell-BP caused the paper disruption.

In a second step, CMC-BP papers were impregnated with dodecyl methacrylate and irradiated with UV light. The presence of benzophenone functionalities allowed the polymerization of poly(dodecyl methacrylate) on the paper surface. The polymer did not modify the visual aspect of the paper. Nevertheless, poly(dodecyl methacrylate)-modified CMC-BP papers changed their behavior from hydrophilic to hydrophobic. Thus, when a droplet of water was in contact with the paper, in the case of starting CMC-BP papers, water was completely adsorbed by the paper. On the contrary, when CMC-BP papers were modified by poly(dodecyl methacrylate), the contact angle was $106 \pm 8°$ (Figure 7). This value was in agreement with pure poly(dodecyl methacrylate) films, which showed a contact angle around 110°.[54] Polymerization at the cellulose surface favored water repelling and prevented the water penetration in the paper structure, which explained

the higher contact angle values. Compared to modified cellulose papers, for example, by the adsorption of poly-(styrene) or poly(trifluoroethylene), the CMC-BP papers reached similar values to poly(trifluoroethylene) adsorbed at a high concentration (above 1 g L^{-1}).[55] The advantage of the surface grafting relied on low diffusion of the hydrophobic polymer inside the cellulose network and the good surface coverage.

The chemical grafting of poly(dodecyl methacrylate) by the benzophenone functionalities on the cellulose surface allowed the hydrophobization of the papers. These results clearly demonstrated the advantages of bifunctionalization, in this work, the concomitant fibrillation, and the possibility of synthesizing hydrophobic polymers at the benzophenone functionality. The presence of both functionalities on the same fiber provides properties that were not achieved by the mixture of monofunctionalized fibers. From a more applicative point of view, the introduction of two functionalities could generate a wide range of cellulose materials (fibers, microfibers, or nanofibers or soluble cellulose) displaying tailored functionalities for specific applications. Despite the advantages of one-pot cellulose multifunctionalization, there are very few examples in literature. Kaldéus et al.[36] introduced carboxymethyl and allyl or alkyne on cellulose fibers; however, their protocol involves two successive Williamson's etherifications to achieve a total charge density of 0.5−0.6 mmol g^{-1} and a DS of allyl and alkyne functionalities around 0.02. Sichinga et al.[56] performed sequential carboxymethylation, periodate oxidation, and Schiff base reactions to obtain imine carboxymethyl dialdehyde modified cellulose fibers. The authors used limited amounts of the oxidant (NaIO$_4$), and reactions were performed without isolating the products, with minor purification steps (decantation). The three reactions must be carried out sequentially because periodate decomposes at the temperatures of carboxymethylation (55 °C). In a different work, Pettignano et al.[44] obtained multifunctional cellulose by periodate oxidation followed by cascade reactions including the Passerini multi-component reaction. They succeeded in simultaneously introducing a *t*-butyl group and a methacrylic acid or a 4-pentynoic acid at the aldehyde groups created by periodate oxidation. The obtained DS was high, from 0.04 to 0.11, for both functionalities (methacrylic acid or 4-pentynoic acid), and it depended on the molar ratios of the chemicals and the degree of oxidation obtained by the previous periodate oxidation step. Our protocol allowed the introduction of two functionalities in only one step. Williamson's etherification is a versatile strategy to introduce a very wide range of functionalities at the hydroxyl groups. By our protocol, we eliminate the use of ethanol during solvent exchange by simple filtration of the cellulose pulp, and we successfully obtained functionalized microfibrillated cellulose in a one-pot reaction by using reduced amounts of chemicals (1 mmol of MCA and 0.3 mmol of BP by gram of cellulose). We used optimized reaction time (1 h) and temperature (70 °C) to reduce energy and increase DS, which was demonstrated by the gel-like behavior of dispersions obtained simply by magnetic stirring without any further mechanical treatment.[20,36]

■ CONCLUSIONS

In this work, we present a straightforward synthetic route to introduce several functionalities on the cellulose surface in one-pot reactions. We introduced two different functionalities on the cellulose fiber in a 1 h reaction. We demonstrated the
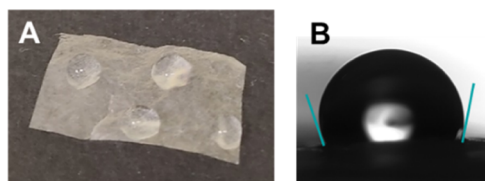

Figure 7. (A) Photograph of the CMC-BP after polymerization of dodecyl methacrylate and (B) representative image of the contact angle of these papers.

successful bifunctionalization by conductometry, FT-IR and solid-state NMR. The simultaneous introduction of negative charge (by the carboxymethyl groups) together with the functionality (benzophenone) facilitated the fiber disruption by soft stirring. Therefore, the application of high energy mechanical treatments such as homogenizer or high pressure microfluidizer would yield functionalized cellulose nanofibers. This is of special importance to enlarge the applications of nanocelluloses, which usually requires tuning the surface properties (hydrophobicity, charge). By carefully selecting the functional groups, we may be able to engineer materials with an unprecedented variety of mechanical properties as well as new functionalities.

■ ASSOCIATED CONTENT

ⓢ Supporting Information

The Supporting Information is available free of charge at https://pubs.acs.org/doi/10.1021/acssuschemeng.2c03754.

> FT-IR of cellulose-BP mixtures and polymerizations and deconvolution of solid-state ^{13}C CP/MAS NMR spectra (PDF)

■ AUTHOR INFORMATION

Corresponding Author

Ana Villares − UR1268 BIA, INRAE, F-44316 Nantes, France; ● orcid.org/0000-0001-5441-7299; Email: ana.villares@inrae.fr

Authors

Céline Moreau − UR1268 BIA, INRAE, F-44316 Nantes, France

Xavier Falourd − UR1268 BIA, INRAE, F-44316 Nantes, France; INRAE, BIBS Facility, F-44316 Nantes, France

Malika Talantikite − UR1268 BIA, INRAE, F-44316 Nantes, France

Bernard Cathala − UR1268 BIA, INRAE, F-44316 Nantes, France; ● orcid.org/0000-0002-3844-872X

Complete contact information is available at: https://pubs.acs.org/10.1021/acssuschemeng.2c03754

Author Contributions

Conceptualization, A.V.; funding acquisition, A.V.; investigation, C.M., XF, M.T., and A.V.; project administration, A.V.; supervision, A.V.; writing—original draft, A.V.; writing—review and editing, C.M., X.F., M.T., B.C., and A.V.

Notes

The authors declare no competing financial interest.

■ ACKNOWLEDGMENTS

■ REFERENCES

(1) Dufresne, A. Nanocellulose: a new ageless bionanomaterial. *Mater. Today* **2013**, *16*, 220−227.

(2) Eichhorn, S. J.; Dufresne, A.; Aranguren, M.; Marcovich, N. E.; Capadona, J. R.; Rowan, S. J.; Weder, C.; Thielemans, W.; Roman, M.; Renneckar, S.; Gindl, W.; Veigel, S.; Keckes, J.; Yano, H.; Abe, K.; Nogi, M.; Nakagaito, A. N.; Mangalam, A.; Simonsen, J.; Benight, A. S.; Bismarck, A.; Berglund, L. A.; Peijs, T. Review: current international research into cellulose nanofibres and nanocomposites. *J. Mater. Sci.* **2010**, *45*, 1−33.

(3) Moon, R. J.; Martini, A.; Nairn, J.; Simonsen, J.; Youngblood, J. Cellulose nanomaterials review: structure, properties and nanocomposites. *Chem. Soc. Rev.* **2011**, *40*, 3941−3994.

(4) Charreau, H.; Cavallo, E.; Foresti, M. L. Patents involving nanocellulose: Analysis of their evolution since 2010. *Carbohydr. Polym.* **2020**, *237*, 116039.

(5) Saito, T.; Yanagisawa, M.; Isogai, A. TEMPO-mediated oxidation of native cellulose: SEC-MALLS analysis of water-soluble and -insoluble fractions in the oxidized products. *Cellulose* **2005**, *12*, 305−315.

(6) Nechyporchuk, O.; Belgacem, M. N.; Bras, J. Production of cellulose nanofibrils: A review of recent advances. *Ind. Crops Prod.* **2016**, *93*, 2−25.

(7) Pääkkö, M.; Ankerfors, M.; Kosonen, H.; Nykänen, A.; Ahola, S.; Österberg, M.; Ruokolainen, J.; Laine, J.; Larsson, P. T.; Ikkala, O.; Lindström, T. Enzymatic hydrolysis combined with mechanical shearing and high-pressure homogenization for nanoscale cellulose fibrils and strong gels. *Biomacromolecules* **2007**, *8*, 1934−1941.

(8) Henriksson, M.; Henriksson, G.; Berglund, L. A.; Lindström, T. An environmentally friendly method for enzyme-assisted preparation of microfibrillated cellulose (MFC) nanofibers. *Eur. Polym. J.* **2007**, *43*, 3434−3441.

(9) Saito, T.; Hirota, M.; Tamura, N.; Kimura, S.; Fukuzumi, H.; Heux, L.; Isogai, A. Individualization of Nano-Sized Plant Cellulose Fibrils by Direct Surface Carboxylation Using TEMPO Catalyst under Neutral Conditions. *Biomacromolecules* **2009**, *10*, 1992−1996.

(10) Saito, T.; Kimura, S.; Nishiyama, Y.; Isogai, A. Cellulose nanofibers prepared by TEMPO-mediated oxidation of native cellulose. *Biomacromolecules* **2007**, *8*, 2485−2491.

(11) Isogai, A.; Saito, T.; Fukuzumi, H. TEMPO-oxidized cellulose nanofibers. *Nanoscale* **2011**, *3*, 71−85.

(12) Isogai, T.; Yanagisawa, M.; Isogai, A. Degrees of polymerization (DP) and DP distribution of cellouronic acids prepared from alkali-treated celluloses and ball-milled native celluloses by TEMPO-mediated oxidation. *Cellulose* **2009**, *16*, 117−127.

(13) Nakamura, Y.; Ono, Y.; Saito, T.; Isogai, A. Characterization of cellulose microfibrils, cellulose molecules, and hemicelluloses in buckwheat and rice husks. *Cellulose* **2019**, *26*, 6529−6541.

(14) Saito, T.; Isogai, A. Ion-exchange behavior of carboxylate groups in fibrous cellulose oxidized by the TEMPO-mediated system. *Carbohydr. Polym.* **2005**, *61*, 183−190.

(15) Ambjornsson, H. A.; Schenzel, K.; Germgard, U. Carboxymethyl Cellulose Produced at Different Mercerization Conditions and Characterized by NIR FT Raman Spectroscopy in Combination with Multivariate Analytical Methods. *Bioresources* **2013**, *8*, 1918−1932.

(16) Harding, R. B.; Crenshaw, S. L. H.; Gregory, P. E.; Broughton, D. H. Cellulose ethers and method of preparing the same. EP 1230456 B1, 2004.

(17) Reinhardt, R. M.; Fenner, T. W.; Reid, J. D. The nonaqueous carboxymethylation of cotton. *Text. Res. J.* **1957**, *27*, 873−878.

(18) Wågberg, L.; Decher, G.; Norgren, M.; Lindström, T.; Ankerfors, M.; Axnäs, K. The build-up of polyelectrolyte multilayers of microfibrillated cellulose and cationic polyelectrolytes. *Langmuir* **2008**, *24*, 784−795.

(19) Bidgoli, H.; Zamani, A.; Taherzadeh, M. J. Effect of carboxymethylation conditions on the water-binding capacity of chitosan-based superabsorbents. *Carbohydr. Res.* **2010**, *345*, 2683−2689.

(20) Im, W.; Lee, S.; Rajabi Abhari, A. R.; Youn, H. J.; Lee, H. L. Optimization of carboxymethylation reaction as a pretreatment for production of cellulose nanofibrils. *Cellulose* **2018**, *25*, 3873−3883.

(21) Cunha, A. G.; Mougel, J. B.; Cathala, B.; Berglund, L. A.; Capron, I. Preparation of Double Pickering Emulsions Stabilized by Chemically Tailored Nanocelluloses. *Langmuir* **2014**, *30*, 9327−9335.

(22) Sekine, Y.; Nankawa, T.; Yunoki, S.; Sugita, T.; Nakagawa, H.; Yamada, T. Eco-friendly Carboxymethyl Cellulose Nanofiber Hydrogels Prepared via Freeze Cross-Linking and Their Applications. *ACS Appl. Polym. Mater.* **2020**, *2*, 5482−5491.

(23) Beck, S.; Méthot, M.; Bouchard, J. General procedure for determining cellulose nanocrystal sulfate half-ester content by conductometric titration. *Cellulose* **2015**, *22*, 101−116.

(24) Moreau, C.; Tapin-Lingua, S.; Grisel, S.; Gimbert, I.; Le Gall, S.; Meyer, V.; Petit-Conil, M.; Berrin, J. G.; Cathala, B.; Villares, A. Lytic polysaccharide monooxygenases (LPMOs) facilitate cellulose nanofibrils production. *Biotechnol. Biofuels* **2019**, *12*, 156.

(25) Villares, A.; Moreau, C.; Bennati-Granier, C.; Garajova, S.; Foucat, L.; Falourd, X.; Saake, B.; Berrin, J. G.; Cathala, B. Lytic polysaccharide monooxygenases disrupt the cellulose fibers structure. *Sci. Rep.* **2017**, *7*, 40262.

(26) Newman, R. H. Estimation of the lateral dimensions of cellulose crystallites using NMR signal strengths. *Solid State Nucl. Magn. Reson.* **1999**, *15*, 21−29.

(27) Palme, A.; Idström, A.; Nordstierna, L.; Brelid, H. Chemical and ultrastructural changes in cotton cellulose induced by laundering and textile use. *Cellulose* **2014**, *21*, 4681−4691.

(28) Wickholm, K.; Larsson, P. T.; Iversen, T. Assignment of noncrystalline forms in cellulose I by CP/MAS 13C NMR spectroscopy. *Carbohydr. Res.* **1998**, *312*, 123−129.

(29) Schwanninger, M.; Rodrigues, J. C.; Pereira, H.; Hinterstoisser, B. Effects of short-time vibratory ball milling on the shape of FT-IR spectra of wood and cellulose. *Vib. Spectrosc.* **2004**, *36*, 23−40.

(30) da Silva Perez, D. D.; Montanari, S.; Vignon, M. R. TEMPO-mediated oxidation of cellulose III. *Biomacromolecules* **2003**, *4*, 1417−1425.

(31) Bait, S.; Shinde, S.; Adivarekar, R.; Sekar, N. Multifunctional properties of benzophenone based acid dyes: Synthesis, spectral properties and computational study. *Dyes Pigm.* **2020**, *180*, 108420.

(32) Zhao, Y.; Dan, Y. Synthesis and characterization of a polymerizable benzophenone derivative and its application in styrenic polymers as UV-stabilizer. *Eur. Polym. J.* **2007**, *43*, 4541−4551.

(33) Kolev, T. M.; Stamboliyska, B. A. Vibrational spectra and structure of benzophenone and its 18O and d10 labelled derivatives: an ab initio and experimental study. *Spectrochim. Acta, Part A* **2000**, *56*, 119−126.

(34) Li, X. H.; Gong, X. Y.; Zhang, X. Z. Molecular structure and vibrational spectra of Benzophenone hydrazone molecule by density functional theory. *Comput. Theor. Chem.* **2011**, *976*, 191−196.

(35) Oh, S. Y.; Yoo, D. I.; Shin, Y.; Kim, H. C.; Kim, H. Y.; Chung, Y. S.; Park, W. H.; Youk, J. H. Crystalline structure analysis of cellulose treated with sodium hydroxide and carbon dioxide by means of X-ray diffraction and FTIR spectroscopy. *Carbohydr. Res.* **2005**, *340*, 2376−2391.

(36) Kaldéus, T.; Larsson, P. T.; Boujemaoui, A.; Malmström, E. One-pot preparation of bi-functional cellulose nanofibrils. *Cellulose* **2018**, *25*, 7031−7042.

(37) Larsson, P. T.; Hult, E. L.; Wickholm, K.; Pettersson, E.; Iversen, T. CP/MAS -NMR spectroscopy applied to structure and interaction studies on cellulose I. *Solid State Nucl. Magn. Reson.* **1999**, *15*, 31−40.

(38) Larsson, P. T.; Wickholm, K.; Iversen, T. A CP/MAS C-13 NMR investigation of molecular ordering in celluloses. *Carbohydr. Res.* **1997**, *302*, 19−25.

(39) Kono, H.; Yunoki, S.; Shikano, T.; Fujiwara, M.; Erata, T.; Takai, M. CP/MAS 13C NMR Study of Cellulose and Cellulose Derivatives. 1. Complete Assignment of the CP/MAS 13C NMR Spectrum of the Native Cellulose. *J. Am. Chem. Soc.* **2002**, *124*, 7506−7511.

(40) Moradian, M.; Islam, M. S.; van de Ven, T. G. M. Insoluble Regenerated Cellulose Films Made from Mildly Carboxylated Dissolving and Kraft Pulps. *Ind. Eng. Chem. Res.* **2021**, *60*, 5385−5393.

(41) Guigo, N.; Mazeau, K.; Putaux, J.-L.; Heux, L. Surface modification of cellulose microfibrils by periodate oxidation and subsequent reductive amination with benzylamine: a topochemical study. *Cellulose* **2014**, *21*, 4119−4133.

(42) Dais, P. Conformational Properties of para Monosubstituted Benzophenones. 13C NMR and Molecular Modeling Studies. *Z. Phys. Chem.* **1990**, *168*, 43−53.

(43) Espino-Pérez, E.; Domenek, S.; Belgacem, N.; Sillard, C.; Bras, J. Green Process for Chemical Functionalization of Nanocellulose with Carboxylic Acids. *Biomacromolecules* **2014**, *15*, 4551−4560.

(44) Pettignano, A.; Leguy, J.; Heux, L.; Jean, B.; Charlot, A.; Fleury, E. Multifunctionalization of cellulose microfibrils through a cascade pathway entailing the sustainable Passerini multi-component reaction. *Green Chem.* **2020**, *22*, 7059−7069.

(45) Kono, H.; Oshima, K.; Hashimoto, H.; Shimizu, Y.; Tajima, K. NMR characterization of sodium carboxymethyl cellulose: Substituent distribution and mole fraction of monomers in the polymer chains. *Carbohydr. Polym.* **2016**, *146*, 1−9.

(46) Capitani, D.; Porro, F.; Segre, A. L. High field NMR analysis of the degree of substitution in carboxymethyl cellulose sodium salt. *Carbohydr. Polym.* **2000**, *42*, 283−286.

(47) Daicho, K.; Kobayashi, K.; Fujisawa, S.; Saito, T. Crystallinity-Independent yet Modification-Dependent True Density of Nanocellulose. *Biomacromolecules* **2020**, *21*, 939−945.

(48) Hult, E. L.; Larsson, P. T.; Iversen, T. Cellulose fibril aggregation - an inherent property of kraft pulps. *Polymer* **2001**, *42*, 3309−3314.

(49) Nishiyama, Y.; Kim, U.-J.; Kim, D.-Y.; Katsumata, K. S.; May, R. P.; Langan, P. Periodic Disorder along Ramie Cellulose Microfibrils. *Biomacromolecules* **2003**, *4*, 1013−1017.

(50) Sanai, Y.; Kagami, S.; Kubota, K. Cross-linking photo-polymerization of monoacrylate initiated by benzophenone. *J. Polym. Sci., Part A: Polym. Chem.* **2018**, *56*, 1545−1553.

(51) Zoppe, J. O.; Ataman, N. C.; Mocny, P.; Wang, J.; Moraes, J.; Klok, H. A. Surface-Initiated Controlled Radical Polymerization: State-of-the-Art, Opportunities, and Challenges in Surface and Interface Engineering with Polymer Brushes. *Chem. Rev.* **2017**, *117*, 1105−1318.

(52) Zoppe, J. O.; Xu, X. Y.; Känel, C.; Orsolini, P.; Siqueira, G.; Tingaut, P.; Zimmermann, T.; Klok, H. A. Effect of Surface Charge on Surface-Initiated Atom Transfer Radical Polymerization from Cellulose Nanocrystals in Aqueous Media. *Biomacromolecules* **2016**, *17*, 1404−1413.

(53) Xiao, C. M.; Li, H. Q.; Gao, Y. K. Preparation of fast pH-responsive ferric carboxymethylcellulose/poly(vinyl alcohol) double-network microparticles. *Polym. Int.* **2009**, *58*, 112−115.

(54) Okouchi, M.; Yamaji, Y.; Yamauchi, K. Contact Angle of Poly(alkyl methacrylate)s and Effects of the Alkyl Group. *Macromolecules* **2006**, *39*, 1156−1159.

(55) Kontturi, K. S.; Biegaj, K.; Mautner, A.; Woodward, R. T.; Wilson, B. P.; Johansson, L. S.; Lee, K. Y.; Heng, J. Y. Y.; Bismarck, A.; Kontturi, E. Noncovalent Surface Modification of Cellulose Nanopapers by Adsorption of Polymers from Aprotic Solvents. *Langmuir* **2017**, *33*, 5707−5712.

(56) Sichinga, M. C.; Kline, T.; Whitehead, M. A.; van de Ven, T. G. M. One-pot eco-friendly oxidative synthesis of imine carboxymethyl dialdehyde cellulosic fibers. *Cellulose* **2022**, *29*, 799−815.